Calculation of transient tube-wave signals in cross-borehole acoustics

Adrianus T. de Hoop,[a] Bastiaan P. de Hon,[a] and Andrew L. Kurkjian[b]
Schlumberger Cambridge Research, Cambridge CB3 0HG, England

(Received 24 March 1993; revised 31 October 1993; accepted 4 November 1993)

Closed-form expressions are obtained for the transient acoustic pressure in a borehole, due to the action of a volume injection (acoustic monopole) source in another borehole in a typical cross-well seismic setting with a homogeneous isotropic solid formation. At the relatively low frequencies involved the acoustic wave motion inside a fluid-filled borehole, which may be surrounded by a structure of perfectly bonded circularly cylindrical solid shells, is dominated by tube waves. The excitation and propagation properties of the tube wave are modeled by regarding the borehole as an acoustic waveguide with a compliant inner wall. The corresponding elastic wave-field quantities at the outer borehole wall are evaluated through a plane-strain elastostatic transfer of the stress and the elastic displacement across the shell structure. For the radiation of the wave-field quantities into the formation, the elastodynamic Kirchhoff–Huygens integral representation is used. The acoustic pressure on the axis of the receiving borehole is evaluated with the aid of the fluid/solid acoustic reciprocity theorem. Various physical phenomena are described by the resulting expressions, including pre- and postcritical phenomena (conical waves) for slow formations, and tunnelinglike phenomena for proximate boreholes in fast formations.

PACS numbers: 43.20.Mv, 43.20.Jr, 43.20.Gp, 43.40.Ph

INTRODUCTION

White and Sengbush[1] were the first to recognize that the measured acoustic signals obtained from cross-hole seismic experiments involving volume injection sources and/or acoustic pressure receivers contain strong tube-wave–related phenomena. For instance, in so-called slow formations where the tube-wave speed exceeds the shear-wave speed in the solid formation, a tube wave propagating along a borehole excites strong conical S waves in the formation. With the recent advances in the area of cross-well seismic data acquisition, strong conical waves have repeatedly been reported. De Bruin and Huizer[2] have presented perhaps the most striking experimental observations of this phenomenon. Cheng *et al.*[3] observed conical waves in a controlled laboratory experiment. Other examples of the strong influence of tube waves on the cross-hole transfer of acoustic signals are given by Albright and Johnson,[4] Worthington,[5] Lines *et al.*,[6] and Krohn,[7] who observed a notable mode conversion from tube waves along vertical boreholes into guided channel waves along horizontal layers in the solid formation.

To model the acoustic radiation from a fluid-filled borehole, various techniques have been presented, which may roughly be categorized by discerning between direct and hybrid modeling methods.

In the *direct modeling methods* one solves the differential equations governing the acoustic wave motion in the borehole fluid and in the solid formation simultaneously. For example, Lee and Balch[8] used the frequency axial-wave-number integration technique. By considering a low-frequency approximation, they retained the dominant tube-wave terms only and performed the wave-number integration using the method of steepest descent, so as to obtain a far-field asymptotic representation for the space-time-domain particle displacement in a fast formation. Meredith[9] performed the frequency axial-wave-number integrations numerically. He also derived a uniform asymptotic representation for the frequency-domain far-field particle displacement. From this asymptotic representation, which is valid for both slow and fast formations, he extracted qualitative information about the behavior of conical waves.

Many authors have generalized the technique of Lee and Balch.[8] For instance, Lee *et al.*[10] incorporated the secondary radiation from totally reflected tube waves at the bottom of a borehole; the far-field radiation patterns for fast formations they thus obtained agreed with the primary and secondary radiation patterns observed in a VSP experiment. Lee[11] investigated nonaxisymmetric solutions for the acoustic wave motion in fast formations, while Winbow[12] modeled the influence of different source types and the presence of a borehole casing.

Finite difference methods have been implemented by Track and Daube,[13] who addressed the full cross-borehole wave propagation problem in slow and fast formations and by Cheng *et al.*[3] who focused their investigation on the coupling of the acoustic wave motion in the borehole fluid to conical P and S waves in a slow formation.

[a]On leave from Delft University of Technology, Department of Electrical Engineering, Laboratory of Electromagnetic Research, P.O. Box 5031, 2600 GA Delft, The Netherlands.
[b]Presently at Schlumberger Well Services, 5000 Gulf Freeway, P.O. Box 2175, Houston, TX 77252-2175.

 0001-4966/94/95(4)/1773/17/$6.00

In the *hybrid modeling methods* one treats the acoustic wave motion in the borehole fluid and in the solid formation separately, by applying some *a priori* knowledge about the problem. For instance, White and Sengbush[1] recognized that, at low frequencies, the tube wave dominates the acoustic wave motion in the borehole fluid. Subsequently, they introduced the notion of moving sources to model the acoustic tube-wave radiation into the formation, using Heelan's[14] far-field expressions for the acoustic radiation due to a transient pressure applied on a circular cylinder of finite extent. They considered the acoustic wave radiation into fast formations only.

Ben-Menahem and Kostek[15] employed a fixed system of equivalent seismic sources to mimic the influence of the borehole on the acoustic wave motion, by matching its far-field radiation characteristics to the far-field radiation characteristics of a fluid-filled borehole in a fast formation obtained by Lee and Balch.[8] Kurkjian and co-workers[16,17] generalized this approach by replacing the radiating source borehole by a moving system of effective seismic sources so as to account for the conical *S*-wave radiation into slow formations. Furthermore, they employed a frequency lateral wave-number integration code to determine the seismic wave-field quantities in the formation. Gibson[18] also employed a moving system of effective seismic sources and calculated the wave-field quantities in slow and fast formations using ray asymptotics.

As to the calculation of the acoustic wave motion induced in the fluid-filled borehole by incident seismic waves, we may again distinguish between direct and hybrid modeling. Schoenberg[19] directly determined the total acoustic wave motion inside the borehole and in its vicinity as it is induced by the passage of a plane elastic wave incident on the borehole from the surrounding slow or fast formation. Boelle, Dietrich, and Paternoster[20] combined Schoenberg's formulation with the asymptotic theory as it was described by Meredith[9] to obtain expressions for the cross-borehole coupling of acoustic waves, valid in both slow and fast formations. Kurkjian and co-workers[16,17] used a hybrid technique, invoking the principle of reciprocity to calculate the space-time-domain acoustic pressure inside a receiving borehole due to seismic waves that emanate from a source borehole. Their technique effectively comes down to superimposing the contributions of effective seismic sources and receivers and describes the cross-borehole coupling of acoustic waves for slow and fast formations.

In this paper, we present a method by which the transfer of transient tube-wave signals in cross-borehole experiments can completely be calculated in closed form. These solutions can serve as an independent check against the results obtained with the aid of alternative methods in which a larger part of the analysis is carried out numerically. One of the advantages of the method presented here is that physical phenomena such as conical refraction and tunneling can be attributed to specific terms in the final closed-form expressions.

The basic assumption in the present method is that the travel times of the elastic waves in the formation over distances of the order of a borehole diameter may be neglected or, equivalently, that the characteristic wavelengths involved are considerably longer than a borehole diameter. No further assumptions are made and, hence, our analysis is not restricted to far-field effects. As a consequence, near-field tunnelinglike phenomena are included. Furthermore, both cased and uncased boreholes are considered.

We first perform the analysis in the complex-frequency or time-Laplace-transform domain and use the *a priori* knowledge that in the low-frequency regime the axisymmetric wave motion in the borehole fluid is dominated by tube waves. After that we perform a closed-form inversion to the time domain by inspection. Consecutively, we discuss the propagation properties of the tube wave, which depend on the radial stiffness of the inner borehole wall, the excitation of a tube wave by a point source of volume injection, and the influence of the presence of a concentric shell structure surrounding the borehole fluid on the radial stiffness of the inner wall and on the resulting wave-field quantities at the outer wall.

Next, we let the values of the wave-field quantities at the outer wall serve as the surface sources that generate the acoustic wave field in the homogeneous solid formation according to the Kirchhoff–Huygens representation theorem.

We employ a fluid/solid reciprocity theorem to evaluate the acoustic pressure as it is induced inside a receiving borehole by an incident seismic wave field. Combining these results, we obtain an analytical expression for the acoustic pressure on the axis of a receiving borehole, due to the action of a point source on the axis of a source borehole. After the transformation back to the space-time domain, we arrive at the transient Green's function for the cross-hole transient signal transfer. The resulting expressions are set against the corresponding far-field asymptotic expressions and illustrated with the results of numerical simulations. We conclude this paper with a discussion about the ramifications of the presented theory and results.

I. DESCRIPTION OF THE CONFIGURATION AND FORMULATION OF THE PROBLEM

We investigate theoretically the signal transfer through a configuration consisting of two parallel, circularly cylindrical, fluid-filled boreholes embedded in a perfectly elastic, homogeneous, isotropic solid formation. To specify the position in the configuration, we employ the coordinates $\{x_1,x_2,x_3\}$ with respect to a fixed, orthogonal, Cartesian frame of reference, with the origin $\mathcal{O}$ and the three mutually perpendicular base vectors $\{\mathbf{i}_1,\mathbf{i}_2,\mathbf{i}_3\}$ of unit length each. In the indicated order, the base vectors form a right-handed system. In accordance with the geophysical convention, $\mathbf{i}_3$ points vertically downward. The subscript notation for Cartesian vectors and tensors is used. Lowercase Latin subscripts are used for this purpose; they are to be assigned the values 1, 2, and 3. Whenever necessary, lowercase Greek subscripts are used to indicate the horizontal components of the Cartesian vectors and tensors; they are to be assigned the values 1 and 2. For the vertical component the subscript 3 is then written explicitly. To all repeated subscripts, the summation convention applies.

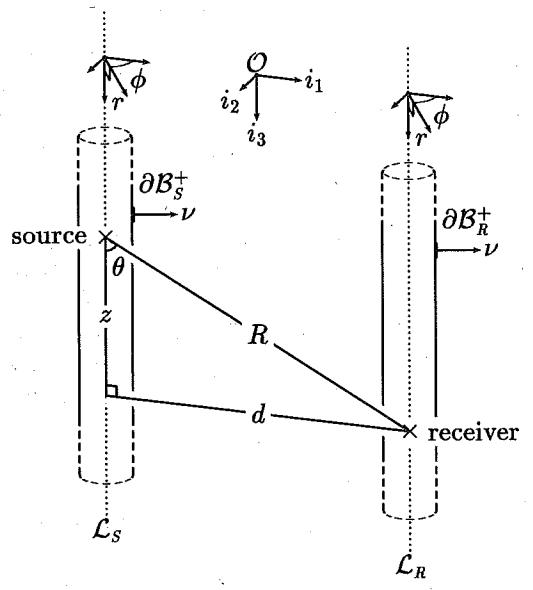

FIG. 1. Depiction of the configuration.

The subscripts r, ϕ, and z are reserved ones to be used in local circularly cylindrical coordinate systems in the boreholes, with the z axes coinciding with the pertaining borehole axes. Whenever appropriate, the position is also specified by the position vector $\mathbf{x}=x_p\mathbf{i}_p$. The time coordinate is denoted by t. Partial differentiation with respect to x_p is denoted by ∂_p; ∂_t is a reserved symbol denoting partial differentiation with respect to time. Integration with respect to time is denoted by the symbol I_t.

At the instant $t=0$, a point source of volume injection, located at $\mathbf{x}=\mathbf{x}^S$ on the axis of the source borehole, starts to generate the acoustic wave motion, which is measured by an acoustic pressure point receiver located at $\mathbf{x}=\mathbf{x}^R$ on the axis of the receiving borehole. The domains occupied by the fluid columns inside the source and receiving boreholes are denoted as $\mathscr{B}_S^-$ and $\mathscr{B}_R^-$, while $b_{S;R}^-$ and $\Omega_{S;R}^-$ denote the pertaining radii and cross-sectional areas, respectively. In between the fluid columns and the solid formation a finite system of concentric circularly cylindrical shells, representing casing, cementing, etc., may be present. The domains occupied by the source and receiving holes, including these shells, are denoted as $\mathscr{B}_S^+$ and $\mathscr{B}_R^+$, while $b_{S;R}^+$ and $\Omega_{S;R}^+$ denote the pertaining radii and cross-sectional areas, respectively. The different layers in the shell structure are assumed to be perfectly bonded to one another and to the solid formation. The fluid/solid interfaces in the source and receiving boreholes are denoted as $\partial\mathscr{B}_S^-$ and $\partial\mathscr{B}_R^-$, respectively; the interfaces between the outermost shells of the source and receiving holes and the formation are denoted as $\partial\mathscr{B}_S^+$ and $\partial\mathscr{B}_R^+$, respectively. The unit vector $\boldsymbol{\nu}$ is oriented along the outward normal to the interfaces, i.e., into the formation. Further, $\mathscr{L}_S$ and $\mathscr{L}_R$ are used to indicate the borehole axes of the source and receiving boreholes, respectively. The configuration is shown in Fig. 1.

The vector $(\mathbf{x}^R-\mathbf{x}^S)$ has the components $(d,0,z)$, in which d and z are the horizontal and vertical offsets of the receiver with respect to the source, respectively. Further, we employ the spherical polar coordinates R and θ, where $d=R\sin(\theta)$ and $z=R\cos(\theta)$, in which θ is the angle between the vector $(\mathbf{x}^R-\mathbf{x}^S)$ and the vertical.

The method that we employ consists of the following steps. First, we investigate the acoustic wave motion in the fluid. To this end the transmitting borehole is considered as an acoustic waveguide with a compliant wall. In this borehole a point source of volume injection, i.e., an acoustic monopole source, generates an impulsive wave, which, in the borehole is assumed to be dominated by the tube wave. The transfer of the radial traction and particle velocity across the cylindrical shell structure surrounding the borehole, is calculated via a plane-strain quasistatic stress analysis. The propagation through the formation is accounted for by considering the outer wall of the transmitting borehole as covered by known, radiating moving surface sources and employing the corresponding Kirchhoff–Huygens integral representation, which, in principle, is exact. The transfer of the radiated elastic wave to the tube waves in the receiving borehole is calculated with the aid of the acoustic reciprocity theorem for fluid/solid configurations. The intermediate steps in the analysis are carried out in the complex-frequency domain; the final answer in the time domain follows by inspection.

The linearized equation of motion and the deformation rate equation governing the acoustic wave motion in the borehole fluid in the presence of a point source of volume injection are given by

$$\partial_k p+\rho^f\,\partial_t w_k=0, \tag{1a}$$

$$\partial_k w_k+\kappa^f\,\partial_t p=Q(t)\delta(\mathbf{x}-\mathbf{x}^S), \tag{1b}$$

in which p is the acoustic pressure (Pa), w_m is the particle velocity (m/s), ρ^f is the volume density of mass (kg/m^3), κ^f is the compressibility (Pa^{-1}), and Q is the time rate of volume injection of the point source (m^3/s). The linearized source-free equation of motion and the deformation rate equation governing the wave motion in the solid formation are given by

$$-\Delta_{kmpq}\,\partial_m\tau_{pq}+\rho^s\,\partial_t v_k=0, \tag{2a}$$

$$\Delta_{ijmk}\,\partial_m v_k-S_{ijpq}\,\partial_t\tau_{pq}=0, \tag{2b}$$

in which τ_{pq} is the dynamic stress (Pa), v_k is the particle velocity (m/s), ρ^s is the volume density of mass (kg/m^3), and S_{ijpq} is the compliance (Pa^{-1}). Further, $\Delta_{ijpq}=(\delta_{ip}\delta_{jq}+\delta_{iq}\delta_{jp})/2$ is the completely symmetric unit tensor of rank 4 and δ_{ij} is the Kronecker unit tensor of rank 2. The compliance is the inverse of the stiffness C_{ijpq} (Pa), i.e.,

$$S_{ijpq}C_{pqkm}=\Delta_{ijkm}. \tag{3}$$

For an isotropic solid the stiffness is given by

$$C_{ijpq}=\lambda\delta_{ij}\delta_{pq}+2\mu\Delta_{ijpq}, \tag{4}$$

where λ and μ (Pa) denote the Lamé coefficients.

Our method of analysis involves the use of a unilateral Laplace transformation with respect to time. The

transform-domain quantities are indicated by a diacritical hat. For example, the Laplace transform of the acoustic pressure in the fluid is given by

$$\hat{p}(\mathbf{x},s)=\int_{t=0^-}^{\infty}\exp(-st)p(\mathbf{x},t)dt, \tag{5}$$

in which we take s real and positive and rely on Lerch's theorem for the transformation back to the time domain. As a consequence of the Laplace transformation and the vanishing initial conditions we have $\partial_t \to s$.

II. THE EXCITATION AND PROPAGATION OF THE TUBE WAVE

To keep the notation transparent, we drop, wherever possible, the indices S and R that indicate the source and receiving holes, respectively. Employing circularly cylindrical coordinates, we write the acoustic wave-field quantities pertaining to a rotational axisymmetric axial waveguide mode in the borehole fluid as

$$\{\hat{p},\hat{w}_r,\hat{w}_z\}(r,z,s)=\{\tilde{p},\tilde{w}_r,\tilde{w}_z\}(r,s)\exp(-s\gamma z), \tag{6}$$

in which $\tilde{p}$, $\tilde{w}_r$, and $\tilde{w}_z$ are the modal amplitudes of the acoustic pressure and the radial and vertical components of the particle velocity, respectively, and γ is the modal slowness. Using the axisymmetric Laplace-transformed version of Eq. (1) in circularly cylindrical coordinates together with Eq. (6), we obtain

$$\frac{\partial\tilde{p}}{\partial r}+s\rho^f\tilde{w}_r=0, \tag{7a}$$

$$-s\gamma\tilde{p}+s\rho^f\tilde{w}_z=0, \tag{7b}$$

$$\frac{\partial\tilde{w}_r}{\partial r}+r^{-1}\tilde{w}_r-s\gamma\tilde{w}_z+s\kappa^f\tilde{p}=0. \tag{7c}$$

Writing the modal amplitudes in terms of their Taylor expansions around $r=0$ and retaining only the lowest-order terms, we arrive at the approximate expressions

$$\tilde{p}=\tilde{p}(0), \tag{8a}$$

$$\tilde{w}_z=(\gamma/\rho^f)\tilde{p}, \tag{8b}$$

$$\tilde{w}_r=s[(\gamma^2-c_f^{-2})/2\rho^f]\tilde{p}r, \tag{8c}$$

in which $c_f=(\rho^f\kappa^f)^{-1/2}$ is the acoustic wave speed in the fluid. Let η_w be the radial stiffness at the inner borehole wall to be determined in Sec. III. In terms of this quantity, we have

$$\lim_{r\uparrow b^-}(s\tilde{p}/\tilde{w}_r)=\eta_w. \tag{9}$$

In the quasistatic plane-strain approximation that we consider, the wall stiffness is independent of s. Substitution of Eq. (8) into Eq. (9) leads to the relation

$$\gamma^2-c_f^{-2}=2\rho^f/\eta_w. \tag{10}$$

The solutions for γ to this equation are $\gamma=\pm\gamma_B$, where

$$\gamma_B=\frac{1}{c_B}=\frac{1}{c_f}\left(1+\frac{2c_f^2\rho^f}{\eta_w}\right)^{1/2}, \tag{11}$$

in which γ_B and c_B denote the tube-wave slowness and wave speed, respectively. Since these quantities are independent of s, we infer that Eq. (9) is reactive in nature, i.e., nonradiating. Furthermore, we introduce the axial modal acoustic wave admittance $Y_B=\gamma_B/\rho^f$, through which

$$\tilde{w}_z=\pm Y_B\tilde{p}. \tag{12}$$

The $\pm$ signs above indicate tube waves propagating in the direction of increasing and decreasing z, respectively.

Now, let a point source that injects fluid volume at the time rate $Q=Q(t)$ be located at the level $z=0$ at the axis of the borehole. The causal tube waves propagating away from the source level in the direction of decreasing and increasing z are described by

$$\{\hat{p},\hat{w}_z\}=\begin{cases}\tilde{p}^-\{1,-Y_B\}\exp(sz/c_B), & \text{for } z<0,\\ \tilde{p}^+\{1,Y_B\}\exp(-sz/c_B), & \text{for } z>0,\end{cases} \tag{13}$$

where $\tilde{p}^-$ and $\tilde{p}^+$ are the corresponding modal pressure amplitudes. The presence of a volume injection source is accounted for by requiring the continuity of the acoustic pressure, while enforcing a jump in the axial volume flow according to

$$\lim_{z\downarrow 0}\hat{p}-\lim_{z\uparrow 0}\hat{p}=0, \tag{14a}$$

$$\lim_{z\downarrow 0}\Omega^-\hat{w}_z-\lim_{z\uparrow 0}\Omega^-\hat{w}_z=\hat{Q}, \tag{14b}$$

where $\Omega^-=\pi(b^-)^2$. Substitution of Eq. (13) into Eq. (14) leads to

$$\tilde{p}^+=\tilde{p}^-=\hat{Q}/2\Omega^-Y_B=\hat{Q}\rho^f c_B/2\Omega^-. \tag{15}$$

It is noted that at a source-free junction the right-hand side of Eq. (14b) vanishes, i.e., both the acoustic pressure and the axial volume flow are continuous across a source-free junction (cf. White[21]). The only problem left is to determine η_w.

III. THE TRANSFER OF ACOUSTIC SIGNALS ACROSS THE BOREHOLE SHELL

Marzetta and Schoenberg[22] have demonstrated that in order to model the propagation of the tube wave along a fluid-filled borehole surrounded by a perfectly bonded concentric shell structure, the influence of the solid shell and formation may be accounted for by using the plane-strain elastostatic approximation for the field in the solid. The nomenclature of the relevant quantities pertaining to the shell structure surrounding the borehole is listed in Table I. To facilitate the calculations, we introduce the elastostatic radial stiffness in the solid defined by

$$\eta=-r\tau_{rr}/u_r, \tag{16}$$

where τ_{rr} and u_r are the elastostatic normal traction and radial particle displacement, respectively.

In the quasistatic plane-strain approximation both the traction and the particle velocity at $\partial\mathscr{B}^+$ are oriented along ν, while the particle velocity is proportional to the traction and to s. Employing Eq. (16) then leads to

$$\Delta_{mjpq}\nu_j\hat{\tau}_{pq}=\hat{\tau}\delta_{m\mu}\nu_\mu, \quad \text{at } \partial\mathscr{B}^+, \tag{17a}$$

TABLE I. Nomenclature pertaining to the shell structure of concentric solid layers that may surround the borehole fluid.

Domain	Radial coordinate $r\in$	Stiffness at inner boundary	Plane strain coefficients
$\mathscr{D}_1$	$(r_1=b^-,r_2)$	$\eta_w=\eta_1$	$A_1;\ B_1$
⋮	⋮	⋮	⋮
$\mathscr{D}_J$	(r_J,r_{J+1})	η_J	$A_J;\ B_J$
$\mathscr{D}_{J+1}$	(r_{J+1},r_{J+2})	η_{J+1}	$A_{J+1};\ B_{J+1}$
⋮	⋮	⋮	⋮
$\mathscr{D}_N$	$(r_N=b^+,\infty)$	$\eta_N=2\mu_N$	$A_N;\ B_N=0$

$$\hat{v}_k=\delta_{k\kappa}\hat{v}_\kappa=-(sb^+/\eta_N)\hat{\tau}\delta_{k\kappa}\nu_\kappa,\quad \text{at } \partial\mathscr{B}^+, \tag{17b}$$

in which $\hat{\tau}$ is the elastodynamic normal traction at the outer wall. Further, the amplitude of the traction is transferred from the inner to the outer borehole wall according to

$$\hat{\tau}=-T\hat{p}, \tag{18}$$

where $\hat{p}$ is the acoustic pressure associated with the tube-wave motion at the inner wall and T is the elastic traction transfer constant.

Via an elastostatic analysis, the radial stiffness at the inner borehole wall, $\eta_w=\eta_1$, and the traction transfer constant are determined from the elastic properties of the given shell structure—if present—and the formation. In Appendix A we present the details of this analysis leading to the recurrence scheme [cf. Eq. (A6)]

$$\begin{aligned}&\eta_N=2\mu_N=2\mu,\\ &B_J=\frac{r_J(2\mu_J-\eta_{J+1})}{r_{J+1}(2\lambda_J+2\mu_J+\eta_{J+1})},\\ &\eta_J=2\frac{\mu_J-(\lambda_J+\mu_J)(r_J/r_{J+1})B_J}{1+(r_J/r_{J+1})B_J},\\ &\quad\text{for } J=N-1,\ldots,1,\end{aligned} \tag{19}$$

and

$$T=\prod_{J=1}^{N-1}\frac{(\lambda_J+\mu_J)B_J-\mu_J(r_J/r_{J+1})}{(\lambda_J+\mu_J)B_J-\mu_J(r_{J+1}/r_J)}, \tag{20}$$

respectively. These results are in accordance with the expressions obtained by Winbow,[12] who used an alternative approach that also applies to the more complicated elastostatic problem of concentric layers with continuously varying elastic properties.

IV. THE RADIATION OF THE TUBE WAVE INTO THE FORMATION

To evaluate the radiated acoustic wave field emanating from the wall of the source borehole into the homogeneous isotropic formation, we employ the elastodynamic Kirchhoff–Huygens integral representation (cf. de Hoop[23,24]).

Through this representation the particle velocity and the acoustic stress are expressed in terms of surface integrals along the outer borehole wall $\partial\mathscr{B}_S^+$ according to

$$\hat{v}_k=\frac{s}{\rho^s}\hat{A}_k-(1/\rho^s)C_{pmij}\,\partial_p\hat{W}_{kmij}, \tag{21a}$$

$$\hat{\tau}_{pq}=(1/s)C_{pqmk}\,\partial_m\hat{v}_k, \tag{21b}$$

in which

$$\hat{A}_k(\mathbf{x})=\int_{\mathbf{x}'\in\partial\mathscr{B}_S^+}\hat{G}_{km}(\mathbf{x}-\mathbf{x}')[-\Delta_{mjpq}\nu_j\hat{\tau}_{pq}](\mathbf{x}')dA \tag{22}$$

is the elastodynamic vector potential associated with the surface forces and

$$\hat{W}_{kmij}(\mathbf{x})=\int_{\mathbf{x}'\in\partial\mathscr{B}_S^+}\hat{G}_{km}(\mathbf{x}-\mathbf{x}')\Delta_{ijpq}\nu_p\hat{v}_q(\mathbf{x}')dA \tag{23}$$

is the elastodynamic tensor potential associated with the time rate of surface deformations. The elastodynamic particle-velocity/force-source Green's tensor is given by

$$\begin{aligned}\hat{G}_{km}(\mathbf{x})=&(1/c_S^2)\delta_{km}\hat{G}_S(\mathbf{x})+(1/s^2)\partial_k\partial_m\\ &\times[\hat{G}_P(\mathbf{x})-\hat{G}_S(\mathbf{x})],\end{aligned} \tag{24}$$

in which

$$\hat{G}_{P,S}(\mathbf{x})=\exp[-s|\mathbf{x}|/c_{P,S}]/4\pi|\mathbf{x}| \tag{25}$$

denotes the scalar Green's functions of the compressional and shear waves and $c_P=[(\lambda+2\mu)/\rho^s]^{-1/2}$ and $c_S=(\mu/\rho^s)^{-1/2}$ denote the compressional and shear wave speeds, respectively.

Upon using Eqs. (17) and (24) and $\eta_N=2\mu$ [cf. Eq. (19)] in Eqs. (22) and (23) and neglecting the travel time across a cross section of the borehole, we can (cf. Appendix B) express the vector and tensor potentials in terms of the scalar compressional- and shear-wave potentials

$$\hat{\Psi}_{P,S}(\mathbf{x})=-\int_{\mathbf{x}'\in\mathscr{L}_S}\hat{G}_{P,S}(\mathbf{x}-\mathbf{x}')\hat{\tau}(x_3')dx_3'. \tag{26}$$

In this procedure an error of $O[s^2(b_S^+)^2/c_S^2+(b_S^+)^2/|\mathbf{x}-\mathbf{x}'|^2]$ is made, which is negligible in many circumstances met in practice. For example, for a characteristic frequency of 400 Hz, a shear wave speed of 3000 m/s, an interwell spacing d of 20 m, and a tube radius of 10 cm, we have $2\pi f b_S^+/c_S=0.084$ and $b_S^+/d=0.005$. Neglecting this error is also consistent with the fact that we have described the acoustic wave motion inside the fluid by considering the nondispersive tube wave only.

The radiated acoustic wave field in the formation thus becomes

$$\begin{aligned}\hat{v}_k(\mathbf{x})=&\frac{\pi(b_S^+)^2 s}{\rho^s}\left[2\left(\frac{1}{c_S^2}\delta_{k3}\,\partial_3-\frac{1}{s^2}\partial_k\partial_3\partial_3\right)\hat{\Psi}_S\right.\\ &\left.+\left(\frac{2}{s^2}\partial_3\partial_3-\frac{1}{c_S^2}\right)\partial_k\hat{\Psi}_P\right],\end{aligned} \tag{27a}$$

$$\hat{\tau}_{pq}(\mathbf{x})=\frac{\pi(b_S^+)^2}{\rho^s}\left[2\frac{\mu}{c_S^2}\left(\delta_{p3}\,\partial_q\partial_3+\delta_{q3}\,\partial_p\partial_3-\frac{2}{s^2}\,\partial_p\partial_q\partial_3\partial_3\right)\hat{\Psi}_S+\left(\frac{2}{s^2}\,\partial_3\partial_3-\frac{1}{c_S^2}\right)\times\left(\lambda\frac{s^2}{c_P^2}\,\delta_{pq}+2\mu\,\partial_p\partial_q\right)\hat{\Psi}_P\right]. \tag{27b}$$

V. THE ACOUSTIC PRESSURE IN THE RECEIVING BOREHOLE

In this section we derive an expression for the acoustic pressure associated with the tube wave, as it is induced in a borehole due to seismic waves that are incident on it from the surrounding formation. The expression is derived with the aid of a suitable application of the reciprocity theorem for acoustic wave fields in fluid/solid configurations (cf. de Hoop[25]). In the reciprocity relation two acoustic states A and B occur. The surface interaction integrals relating these two states for the solid and for the fluid are given by

$$\hat{\mathscr{I}}^s(A,B)=\Delta_{ijpq}\int_{\mathbf{x}\in\partial\mathscr{B}_R^+}(-\hat{\tau}_{pq}^A\hat{v}_i^B+\hat{\tau}_{pq}^B\hat{v}_i^A)\nu_j\,dA, \tag{28a}$$

$$\hat{\mathscr{I}}^f(A,B)=\delta_{ij}\int_{\mathbf{x}\in\partial\mathscr{B}_R^-}(\hat{p}^A\hat{w}_i^B-\hat{p}^B\hat{w}_i^A)\nu_j\,dA, \tag{28b}$$

respectively.

We neglect multiple scattering between the boreholes and take as state A the total wave field in the receiving situation. The total wave field in the formation $\{\hat{\tau}_{pq}^T,\hat{v}_k^T\}$, is written as the linear superposition of an incident wave field $\{\hat{\tau}_{pq}^{\rm in},\hat{v}_k^{\rm in}\}$ and a scattered wave field $\{\hat{\tau}_{pq}^{\rm sc},\hat{v}_k^{\rm sc}\}$, i.e.,

$$\{\hat{\tau}_{pq}^T,\hat{v}_k^T\}=\{\hat{\tau}_{pq}^{\rm in}+\hat{\tau}_{pq}^{\rm sc},\hat{v}_k^{\rm in}+\hat{v}_k^{\rm sc}\}. \tag{29}$$

The corresponding total wave field inside the fluid-filled receiving borehole is $\{\hat{p}^T,\hat{w}_k^T\}$. If the receiving borehole were absent, the incident wave field would be the total wave field in the formation.

As state B, an auxiliary state, we take the acoustic wave field as it would be generated by a point source of volume injection located on the borehole axis where we want to evaluate the received acoustic pressure. The wave-field quantities associated with this auxiliary state in the borehole fluid and in the surrounding solid are denoted as $\{\hat{p}^R,\hat{w}_k^R\}$ and $\{\hat{v}_k^R,\hat{\tau}_{pq}^R\}$, respectively. This auxiliary wave field is the one that would be present in the configuration if the receiving borehole were acting as a transmitting borehole. In Fig. 2 we have schematically depicted the relevant wave fields.

Substitution of Eq. (29) into Eq. (28a) leads to

$$\hat{\mathscr{I}}^s(T,R)=\hat{\mathscr{I}}^s(\text{in},R)+\hat{\mathscr{I}}^s(\text{sc},R). \tag{30}$$

Since multiple scattering effects between the boreholes are neglected, both the scattered and the auxiliary wave fields are source-free and satisfy the causality condition at infinity (outgoing waves). Hence, application of the reciprocity relation relating these two states to the domain outside the receiving borehole yields

$$\hat{\mathscr{I}}^s(\text{sc},R)=0. \tag{31}$$

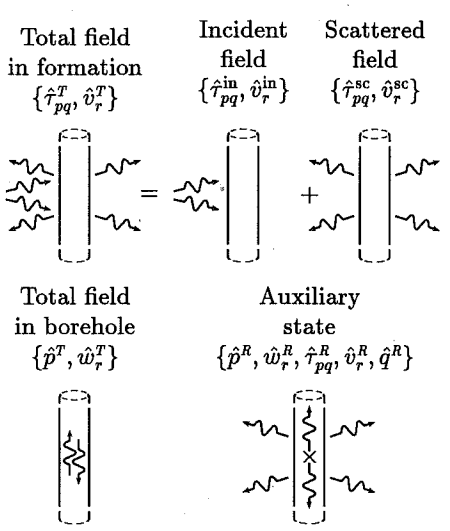

FIG. 2. Schematic depiction of the wave fields that are used in the present application of the fluid/solid reciprocity relation.

In view of the reciprocity of the elastostatic fields in the annular region in between $\partial\mathscr{B}_R^-$ and $\partial\mathscr{B}_R^+$, in both states T and R, and the continuity of the radial traction and the radial particle velocity across the interfaces, we further have

$$\hat{\mathscr{I}}^s(T,R)-\hat{\mathscr{I}}^f(T,R)=0. \tag{32}$$

We use a point source of volume injection located at $\mathbf{x}=\mathbf{x}^R$ on the borehole axis $\mathscr{L}_R$ to generate the auxiliary state, i.e., $\hat{q}^R=\delta(\mathbf{x}-\mathbf{x}^R)$. Then, the reciprocity relation applied to the fluid domain yields

$$\hat{\mathscr{I}}^f(T,R)=\int_{\mathbf{x}\in\partial\mathscr{B}_R^-}\hat{p}^T\hat{q}^R\,dV=\hat{p}^T(\mathbf{x}^R). \tag{33}$$

Upon combining Eqs. (30)–(33) we arrive at the general boundary integral representation of the acoustic pressure at the receiver

$$\hat{p}^T(\mathbf{x}^R)=\hat{\mathscr{I}}^s(\text{in},R)=\Delta_{ijpq}\int_{\mathbf{x}\in\partial\mathscr{B}_R^+}(-\hat{\tau}_{pq}^{\rm in}\hat{v}_i^R+\hat{\tau}_{pq}^R\hat{v}_i^{\rm in})\nu_j\,dA. \tag{34}$$

Now, in the low-frequency limit that we further consider, the auxiliary wave field inside the borehole fluid is dominated by tube waves propagating away from the cross section $x_3=x_3^R$. As a consequence, we may use Eq. (17) to express the wave-field quantities of the auxiliary state in Eq. (34) in terms of $\hat{\tau}^R$, which is the normal traction associated with the tube-wave motion of the auxiliary wave field at the outer wall of the receiving hole. In Appendix C we show that upon neglecting the travel time across a cross section of the borehole, Eq. (34) reduces to the following line integral along the borehole axis:

$$\hat{p}^T(\mathbf{x}^R)=\Omega_R^+\int_{\mathbf{x}\in\mathscr{L}_R}\hat{\tau}^R(x_3)\left(\frac{s}{2\mu}\hat{\tau}^{\mathrm{in}}_{\kappa\kappa}+\partial_\kappa\hat{v}^{\mathrm{in}}_\kappa\right)dx_3, \quad (35)$$

where $\Omega_R^+=\pi(b_R^+)^2$. This approximation is consistent with the one used to obtain Eq. (26). For the homogeneous formation under consideration the stress $\hat{\tau}^{\mathrm{in}}_{pq}$ is related to the particle velocity via Eq. (21b) and, using this relation, Eq. (35) reduces to

$$\hat{p}^T(\mathbf{x}^R)=\Omega_R^+\int_{\mathbf{x}\in\mathscr{L}_R}\hat{\tau}^R(x_3)\left(\frac{c_P^2}{c_S^2}\partial_m\hat{v}^{\mathrm{in}}_m-2\,\partial_3\hat{v}^{\mathrm{in}}_3\right)dx_3. \quad (36)$$

For the cross-hole coupling problem, the value of $\hat{v}^{\mathrm{in}}_k$, needed in Eq. (36), is provided by Eq. (27a). Upon substituting Eqs. (26) and (27a) into Eq. (36) and using Eq. (18) and the property that $\partial_\mu\partial_\mu\hat{G}_{P,S}=(-\partial_3\partial_3+s^2/c_{P,S}^2)\hat{G}_{P,S}$ outside the source point to eliminate all derivatives with respect to the horizontal coordinates, Eq. (36) becomes

$$\hat{p}^T(\mathbf{x}^R)=4\Omega_S^+\Omega_R^+T_ST_R\frac{s}{\rho^s}\times\int_{\mathbf{x}\in\mathscr{L}_R}\int_{\mathbf{x}'\in\mathscr{L}_S}\hat{p}^S(x_3')\hat{p}^R(x_3)\times\left\{\left[\left(\frac{1}{c_S^2}-\frac{1}{s^2}\partial_3\partial_3\right)\partial_3\partial_3\hat{G}_S(\mathbf{x}-\mathbf{x}')\right]+\left[\left(\frac{1}{2c_S^2}-\frac{1}{s^2}\partial_3\partial_3\right)^2s^2\hat{G}_P(\mathbf{x}-\mathbf{x}')\right]\right\}dx_3'\,dx_3, \quad (37)$$

where $T_{S;R}$ and $\hat{p}^{S;R}$ represent the elastic traction transfer constants and the acoustic pressures associated with the tube-wave motion in the source and receiving holes, respectively. To simplify Eq. (37) even further, we need the explicit expressions for the acoustic pressure inside the boreholes, given by [cf. Eqs. (13)–(15)]

$$\hat{p}^S=\frac{\rho_S^fc_{BS}\hat{Q}}{2\Omega_S^-}\left[\exp\left(-\frac{s(x_3-x_3^S)}{c_{BS}}\right)H(x_3-x_3^S)+\exp\left(-\frac{s(x_3^S-x_3)}{c_{BS}}\right)H(x_3^S-x_3)\right], \quad (38a)$$

$$\hat{p}^R=\frac{\rho_R^fc_{BR}}{2\Omega_R^-}\left[\exp\left(-\frac{s(x_3-x_3^R)}{c_{BR}}\right)H(x_3-x_3^R)+\exp\left(-\frac{s(x_3^R-x_3)}{c_{BR}}\right)H(x_3^R-x_3)\right], \quad (38b)$$

in which H denotes the Heaviside unit step function, while c_{BS} and c_{BR} denote the tube-wave speeds in the source and receiving boreholes, respectively.

Taking a closer look at Eqs. (37) and (38), it is apparent that eight basic contributions may be identified, viz., the compressional and shear cross-hole coupling contributions of the down- and upgoing tube waves in the two boreholes, respectively. In Appendix C, Eq. (37) is further unraveled so as to arrive at the final s-domain representation

$$\hat{p}^T(\mathbf{x}^R)=s^2\hat{Q}T_ST_R\frac{\rho_S^f\rho_R^f}{\rho^s}\frac{\Omega_S^+\Omega_R^+}{\Omega_S^-\Omega_R^-}\times\left(\frac{2c_{BS}^2c_{BR}^2}{c_{BS}+c_{BR}}\frac{\hat{h}_P(c_{BS})-\hat{h}_P(c_{BR})}{c_{BS}-c_{BR}}+4s^{-1}\hat{G}_P+\frac{2c_{BS}^2c_{BR}^2}{c_{BS}+c_{BR}}\frac{\hat{h}_S(c_{BS})-\hat{h}_S(c_{BR})}{c_{BS}-c_{BR}}-4s^{-1}\hat{G}_S\right), \quad (39)$$

where the compressional and shear contributions are given by

$$\hat{h}_P(c_B)=c_B^{-3}(c_B^2/2c_S^2-1)^2[\hat{\chi}_P(z,c_B)+\hat{\chi}_P(-z,c_B)], \quad (40a)$$

$$\hat{h}_S(c_B)=c_B^{-3}(c_B^2/c_S^2-1)[\hat{\chi}_S(z,c_B)+\hat{\chi}_S(-z,c_B)], \quad (40b)$$

respectively. In Eq. (40) the compressional and shear single integral constituents

$$\hat{\chi}_{P,S}(z,c_B)=\int_{\zeta=0}^{\infty}\hat{G}_{P,S}(d,0,z-\zeta)\exp\left(-\frac{s\zeta}{c_B}\right)d\zeta, \quad (41)$$

form the elementary building blocks that describe the kinematic aspects of the coupling of a tube wave to the acoustic wave motion at a single point, or vice versa, the coupling of the acoustic wave motion at a single point to a tube wave.

VI. THE SPACE-TIME-DOMAIN ACOUSTIC WAVE MOTION

For the purpose of illustrating the method, we shall derive the time-domain expressions for the acoustic pressure for the general situation in which c_B could exceed both c_S and c_P. It is noted that the situation $c_B>c_P$ is seldom met in practice. However, Cheng *et al.*[3] have conducted a controlled laboratory experiment, using a configuration in which $c_B>c_P$.

The space-time-domain counterpart of $s^{-1}\hat{G}_{P,S}$ is

$$I_tG_{P,S}(d,0,z,t)=H(t-t_{P,S})/4\pi R, \quad (42)$$

where $t_P=R/c_P$ and $t_S=R/c_S$ are the arrival times of the compressional and shear waves, respectively.

In Appendix D, we cast the integral representation of $\hat{\chi}_{P,S}$ given by Eq. (41) in such a form that it can be recognized as a one-sided Laplace transformation of a function of time, which, according to Lerch's theorem, can uniquely be identified with the space-time-domain constituent $\chi_{P,S}$. This leads to

$$\chi_{P,S}(z,c_B)=\begin{cases}\dfrac{2H(t-t_C)-H(t-t_{P,S})}{4\pi[(t-z/c_B)^2-d^2(c_{P,S}^{-2}-c_B^{-2})]^{1/2}},\\ \quad \text{for } c_B>c_{P,S} \text{ and } z/d>\cot(\theta_C),\\ \dfrac{H(t-t_{P,S})}{4\pi[(t-z/c_B)^2-d^2(c_{P,S}^{-2}-c_B^{-2})]^{1/2}},\\ \quad \text{otherwise,}\end{cases} \quad (43)$$

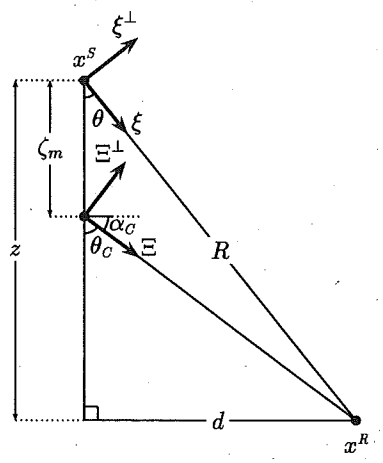

FIG. 3. Depiction of the geometry pertaining to conical waves.

in which $\theta_C=\arccos(c_{P,S}/c_B)$ for $c_B>c_{P,S}$ is related to the angle of conical refraction α_C via $\theta_C=\pi/2-\alpha_C$ (see Fig. 3). In Eq. (39), the constituents $\hat{\chi}_{P,S}(z,c_B)$ and $\hat{\chi}_{P,S}(-z,c_B)$ occur in pairs, and therefore the offset is precritical for $|z/d|<\cot(\theta_C)$ and postcritical for $|z/d|>\cot(\theta_C)$. For precritical offsets conical waves are absent, whereas for postcritical offsets a conical wave precedes the pertaining body wave. The arrival time of a conical wave is found to be

$$t_C=|z|/c_B+d(c_{P,S}^{-2}-c_B^{-2})^{1/2},$$
$$c_B>c_{P,S} \quad \text{and} \quad |z/d|>\cot(\theta_C). \tag{44}$$

Note that for the general case, in which the two tube-wave speeds c_{BS} and c_{BR} exceed both the shear wave speed c_S and the compressional wave speed c_P, there are four (different) angles of conical refraction.

Having determined $G_{P,S}$ and $\chi_{P,S}$, the time-domain representation of the acoustic pressure at the receiver is obtained by replacing s by ∂_t, thus yielding

$$p^T=\partial_t^2 Q(t)\overset{t}{*}g(t), \tag{45}$$

in which $\overset{t}{*}$ denotes a convolution with respect to time, while the cross-well acoustic-pressure/volume-injection-source Green's function is given by

$$g(t)=T_S T_R \frac{\rho_S^f \rho_R^f}{\rho^s}\frac{\Omega_S^+\Omega_R^+}{\Omega_S^-\Omega_R^-}$$
$$\times\left(\frac{2c_{BS}^2c_{BR}^2}{c_{BS}+c_{BR}}\frac{h_P(c_{BS})-h_P(c_{BR})}{c_{BS}-c_{BR}}+4I_tG_P\right.$$
$$\left.+\frac{2c_{BS}^2c_{BR}^2}{c_{BS}+c_{BR}}\frac{h_S(c_{BS})-h_S(c_{BR})}{c_{BS}-c_{BR}}-4I_tG_S\right), \tag{46}$$

where the compressional and shear constituents $h_{P,S}$ are given by

$$h_P(c_B)=c_B^{-3}\left(\frac{c_B^2}{2c_S^2}-1\right)^2[\chi_P(z,c_B)+\chi_P(-z,c_B)], \tag{47a}$$

$$h_S(c_B)=c_B^{-3}\left(\frac{c_B^2}{c_S^2}-1\right)[\chi_S(z,c_B)+\chi_S(-z,c_B)], \tag{47b}$$

respectively. For the particular case in which the tube-wave speeds in the source and receiving boreholes are equal, Eqs. (45) and (46) reduce to

$$p^T=\partial_t^3 Q(t)\overset{t}{*}I_tg(t) \tag{48}$$

and

$$I_tg(t)=T_S T_R\frac{\rho_S^f\rho_R^f}{\rho^s}\frac{\Omega_S^+\Omega_R^+}{\Omega_S^-\Omega_R^-}\left(c_B^3\frac{dI_th_P}{dc_B}+4I_t^2G_P\right.$$
$$\left.+c_B^3\frac{dI_th_S}{dc_B}-4I_t^2G_S\right), \tag{49}$$

respectively. Here, the compressional and shear constituents $I_th_{P,S}$ are given by

$$I_th_P(c_B)=c_B^{-3}\left(\frac{c_B^2}{2c_S^2}-1\right)^2\int_{\tau=-\infty}^{t}[\chi_P(z,c_B)$$
$$+\chi_P(-z,c_B)]d\tau, \tag{50a}$$

$$I_th_S(c_B)=c_B^{-3}\left(\frac{c_B^2}{c_S^2}-1\right)\int_{\tau=-\infty}^{t}[\chi_S(z,c_B)$$
$$+\chi_S(-z,c_B)]d\tau, \tag{50b}$$

respectively. In Eqs. (49) and (50) both the differentiations with respect to the tube-wave speed and integrations with respect to time can be evaluated analytically, but the resulting intricate expressions provide no further insight and are therefore omitted.

Above, we have determined the acoustic pressure in the receiving borehole. Upon replacing the elementary constituents $\chi_{P,S}$ by their asymptotic representations, we obtain a far-field approximation to the acoustic pressure. Note that in Eq. (41), we have represented $\hat{\chi}_{P,S}$ as Laplace integrals. As the asymptotic representations for the elementary constituents, we take the time-domain counterparts of the leading terms of the asymptotic expansions for large s of Eq. (41), which leads to [cf. Eqs. (E3), (E4), (E5), and (E8)]

$$\chi_{P,S}(z,c_B)\sim\begin{cases}\dfrac{H(t-t_C)}{2\pi(2d)^{1/2}(t-t_C)^{1/2}}(c_{P,S}^{-2}-c_B^{-2})^{-1/4}+\dfrac{H(t-t_{P,S})}{4\pi(R/c_B-z/c_{P,S})}, & \text{for } c_B>c_{P,S} \text{ and } z/d>\cot(\theta_C),\\ \dfrac{H(t-t_{P,S})}{4\pi(R/c_B-z/c_{P,S})}, & \text{otherwise,}\end{cases} \tag{51}$$

in which the conical-wave component results from a saddle-point contribution, while the body-wave component results from the contribution of the end point.

VII. NUMERICAL EXAMPLES

The generic expressions for the acoustic pressure inside the receiving borehole are given by Eqs. (42)–(47), while their far-field asymptotic approximations are obtained by replacing Eq. (43) by Eq. (51). All observed phenomena have also been studied by alternative, more numerical methods. The advantage of the present method is that the effects of conical refraction, tunneling, and the like can be attributed to specific terms in our closed-form expressions for the total wave field. To elucidate these expressions and the physical phenomena described by them, we present numerical results pertaining to two different cross-well experiments, one in a slow and one in a fast formation. The distance between the boreholes in both experiments is 20 m. The vertical offsets have been chosen such that the figures optimally display the manifest phenomena. For the source signature $\partial_t^2 Q$ with which the Green's functions are convolved, we take the second derivative of the four-point optimum Blackman–Harris[26] pulse with a pulsewidth of 4 ms.

In the experiments, the point source of volume injection is located on the axis of an uncased borehole, while the receivers are located on the axis of a receiving borehole with a perfectly bonded steel casing. The values of the borehole parameters are listed in Table II. The values of the formation parameters, as well as the resulting tube-wave speeds and traction-transfer constants are listed in Table III. In the figures, the solid lines represent the full closed-form solutions, while the dashed lines represent the far-field asymptotic approximate solutions. We note that through a suitable application of the reciprocity theorem to the far-field asymptotic expressions for the wave-field quantities in a fast formation given by Lee and Balch,[8] we can obtain the equivalent cross-well far-field asymptotic expression for the acoustic pressure in the receiving borehole. In Appendix E we have shown that for fast formations and for precritical offsets in slow formations, this asymptotic expression is in perfect agreement with our asymptotic expression (the dashed lines). The markers with labels *P*, *C*, and *S* indicate the arrivals of the compressional, shear-conical, and shear-body wave, respectively.

Let us first comment on the numerical results pertaining to the cross-well experiment in our slow formation. Since only the tube-wave speed in the receiving borehole exceeds the shear-wave speed, there is but one angle of conical refraction $\alpha_C=64.3$ deg, which for the given inter-well spacing of 20 m corresponds to a critical vertical offset of $z=41.57$ m. In Fig. 4, we have displayed the Green's functions for various pre- and postcritical vertical offsets. The corresponding pressure responses have been displayed in Fig. 5. At zero vertical offset, the leading term of the asymptotic expansion for the shear-wave contribution vanishes, whereas the full expression does yield a nonvanishing contribution. Note that for precritical offsets the Green's functions remain bounded, whereas for postcritical offsets the Green's functions become singular at the arrival time of the conical wave. However, even as the offset changes from pre- to postcritical, the acoustic pressure remains continuous provided that the time rate of volume injection $Q(t)$ is differentiable. Further, we infer from Figs. 4 and 5 that the far-field asymptotic expansion deteriorates near critical offsets, as has already been pointed out by Meredith[9] (p. 104). In order to obtain the correct far-field asymptotic representation near critical offsets, one has to resort to the more sophisticated uniform asymptotic expansions (cf. Meredith,[9] pp. 262–268). However, the asymptotic representation thus obtained is far more complicated than the closed-form analytic expressions given by Eqs. (45)–(50). As the vertical offset is further increased, the shear-conical and shear-body waves eventually split up

TABLE II. Parameter values pertaining to the boreholes.

Physical parameter	Source borehole	Receiving borehole
Fluid wave speed $c^f_{S;R}$ (m/s)	1500	1500
Fluid volume density of mass $\rho^f_{S;R}$(kg/m^3)	1000	1000
Inner radius $b^-_{S;R}$ (cm)		8.89
Outer radius $b^+_{S;R}$ (cm)	10.16	10.16
P wave speed c_P in the casing (m/s)		5750
S wave speed c_S in the casing (m/s)		3120
Casing volume density of mass ρ^s (kg/m^3)		7910

TABLE III. Parameter values pertaining to the slow- and fast-formation experiments.

Physical parameter	Slow formation	Fast formation
P wave speed c_P in the formation (m/s)	2360	4000
S wave speed c_S in the formation (m/s)	1270	2500
Formation density of mass ρ^s (kg/m^3)	2300	2700
Tube wave speed c_{BS} in source hole (m/s)	1183.4	1409.0
Tube wave speed c_{BR} in receiving hole (m/s)	1409.3	1443.8
Source-bore traction-transfer coefficient T_S	1	1
Receiving-bore traction-transfer coefficient T_R	0.179	0.482

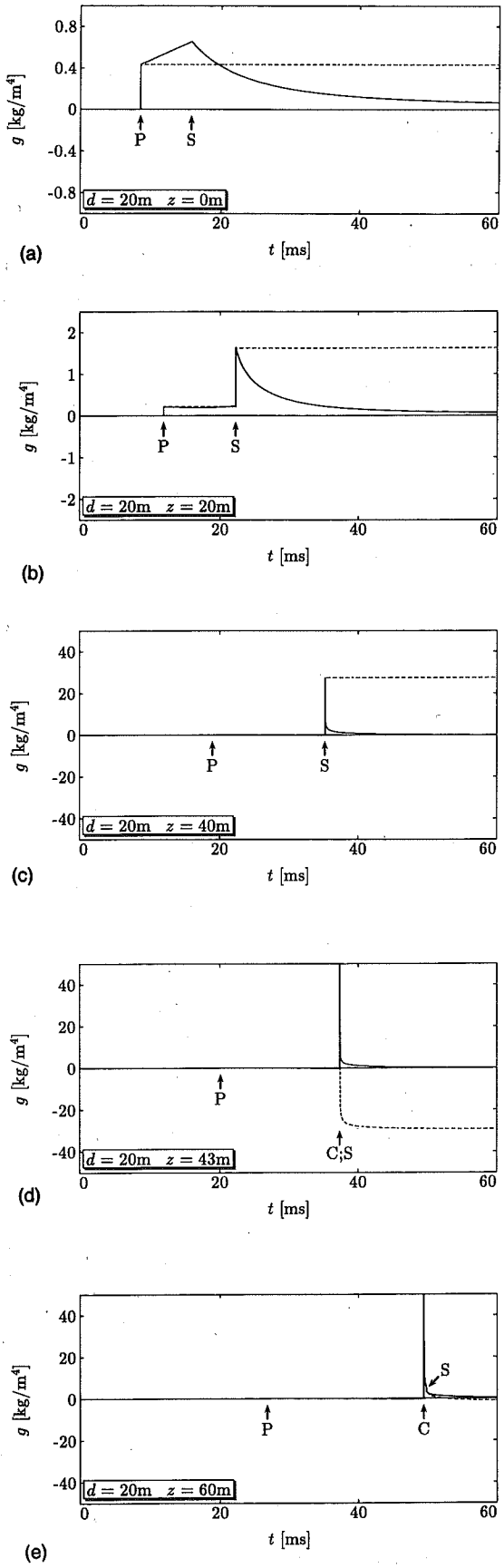

FIG. 4. The cross-well acoustic-pressure/volume-injection-source Green's functions in a slow formation (solid lines) and their far-field asymptotic approximations (dashed lines); for $z > 41.57$ m, the offset is postcritical. The markers with the labels *P*, *C*, and *S* indicate the arrivals of the compressional, shear-conical, and shear-body wave, respectively.

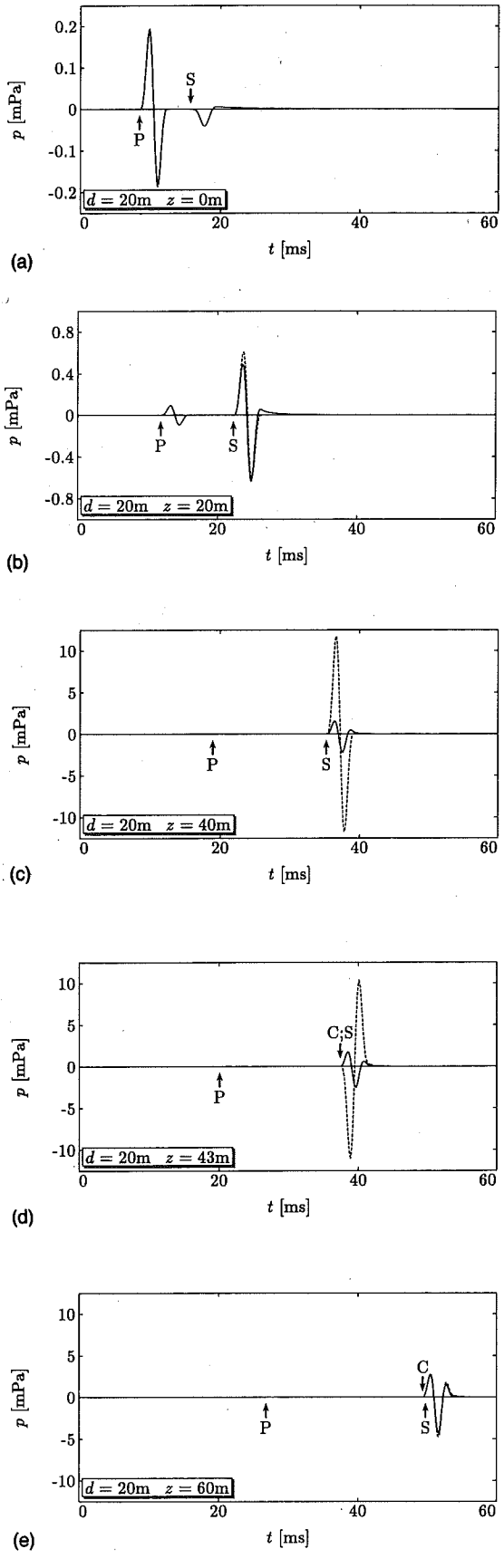

FIG. 5. The acoustic-pressure responses from cross-well experiments in a slow formation (solid lines) and their far-field asymptotic approximations (dashed lines); for $z > 41.57$ m, the offset is postcritical. The markers with the labels *P*, *C*, and *S* indicate the arrivals of the compressional, shear-conical, and shear-body wave, respectively.

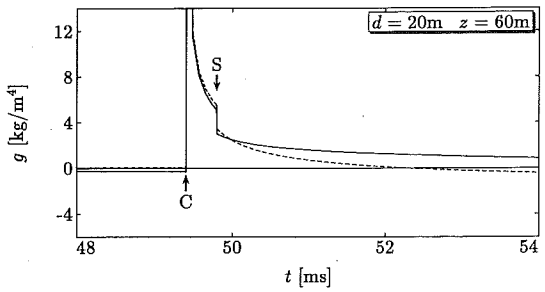

FIG. 6. Enlarged display of the cross-well acoustic-pressure/volume-injection-source Green's function in a slow formation (solid line) and its far-field approximation (dashed line) for a postcritical offset of $z=60$ m. The markers with the labels C and S indicate the arrivals of the shear-conical and shear-body wave, respectively.

into a conical wave with a typical $(t-t_C)^{-1/2}H(t-t_C)$ time behavior of the Green's function and a body wave with a sign-reversed step-function behavior. We have shown the onset of this phenomenon in Fig. 6, where we have displayed the Green's function for a vertical offset of $z=60$ m at an adapted time and amplitude scale.

Next, we comment on the numerical results pertaining to the cross-well experiment in the fast formation. In Fig. 7, we have displayed the Green's functions for two vertical offsets. The corresponding pressure responses have been displayed in Fig. 8. Note that in case the formation is a slow formation rather than a fast formation, the received signal is considerably stronger. The results obtained using far-field asymptotic expressions are, as far as the direct P and S waves are concerned, quite similar to the results obtained using the full expressions. However, if the distance between the two boreholes is of the order of a seismic

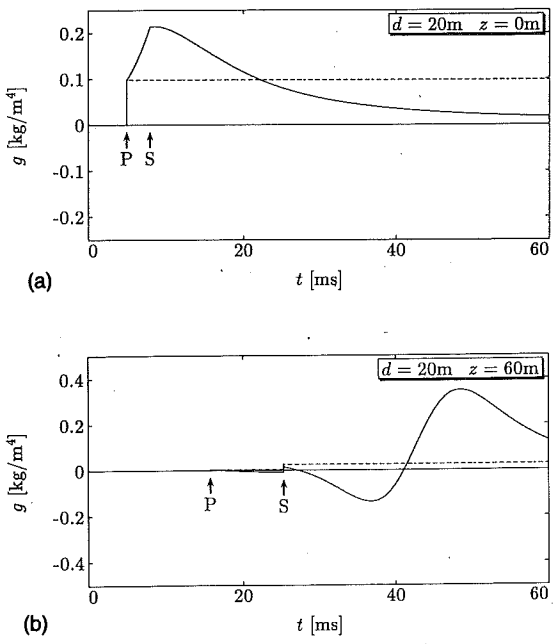

FIG. 7. The cross-well acoustic-pressure/volume-injection-source Green's functions in a fast formation (solid lines) and their far-field asymptotic approximations (dashed lines). The markers with the labels P and S indicate the arrivals of the compressional and shear wave, respectively.

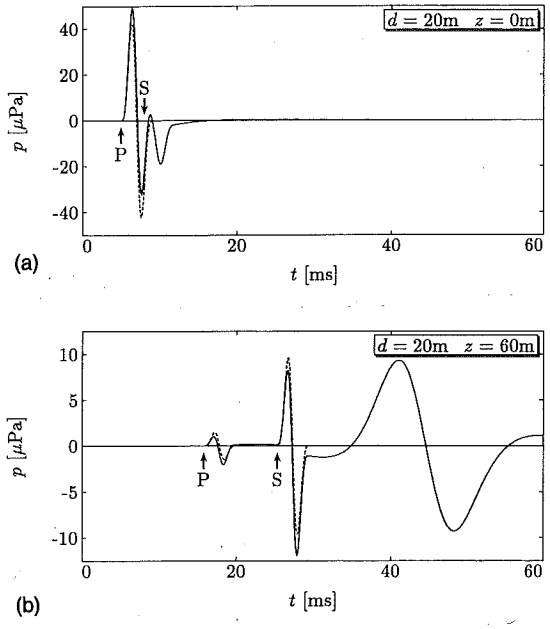

FIG. 8. The acoustic-pressure responses from cross-well experiments in a fast formation (solid lines) and their far-field asymptotic approximations (dashed lines). The markers with the labels P and S indicate the arrivals of the compressional and shear wave, respectively.

wavelength or less, then for large vertical offsets combined P- and S-wave near-field phenomena may dominate the received acoustic signal. In nature these phenomena resemble the effect of tunneling and obviously cannot be obtained using the present far-field asymptotic representation. This is illustrated in Figs. 7 and 8 for a vertical offset of $z=60$ m. Notice the pulse broadening of the received acoustic pressure pulse that is associated with these near-field phenomena.

From the discussion and the figures presented above, we observe that regarding cross-well experiments in slow formations at a postcritical angle, the conical wave forms a prominent contribution to the received acoustic pressure, while regarding cross-well experiments in fast formations at a large vertical offset with the two boreholes being sufficiently close, the near-field phenomena yield a noteworthy contribution to the received acoustic pressure.

VIII. SUMMARY

We have presented closed-form time-domain expressions for the acoustic pressure on the axis of a receiving borehole, due to the action of a point source of volume injection on the axis of a source borehole, on the assumption that the travel times of the elastic waves in the formation over distances of the order of the borehole diameters can be neglected.

To arrive at these results, we have discussed the excitation and propagation of the tube waves, which comprise the dominant part of the acoustic wave motion inside the boreholes [cf. Eqs. (11)–(15)], the quasistatic transfer of the field quantities across the shell structure surrounding the boreholes [cf. Eqs. (16)–(20)], the elastic wave radiation that emanates from the source borehole [cf. Eq. (27)],

and the reception by the receiving borehole of the elastic waves that are incident on it [cf. Eqs. (34)–(41)]. In Eqs. (45)–(50), we have represented the final time-domain closed-form expression in terms of its elementary constituents given by Eqs. (42) and (43), while its far-field asymptotic representation has been obtained by replacing the elementary constituents in Eq. (43) by their corresponding far-field asymptotic representations given by Eq. (51). In Figs. 4–8, we have presented numerical examples, comparing our closed-form expressions represented by the solid lines to the far-field asymptotic representations represented by the dashed lines. Apart from the direct P- and S-wave signals, other physical phenomena that occur in cross-well experiments have been highlighted, such as strong conical waves traveling through slow formations and near-field contributions for large vertical offsets in fast formations.

APPENDIX A: THE QUASISTATIC ELASTIC RADIAL STIFFNESS

In this Appendix, we analyze the elastostatic stress and particle displacement in an annularly piecewise homogeneous isotropic solid in the axisymmetric plane-strain approximation. The corresponding elastostatic particle displacement is written as

$$u_1=u_r(r)\cos(\phi),\quad u_2=u_r(r)\sin(\phi),\quad u_3=0. \tag{A1}$$

Now, consider a composite of N concentric annular domains, including the formation, that are in rigid contact across their interfaces. A schematic description of this configuration is given in Table I. The elastostatic equation of equilibrium for a homogeneous domain in circularly cylindrical coordinates is

$$\frac{\partial\tau_{rr}}{\partial r}+\frac{1}{r}(\tau_{rr}-\tau_{\theta\theta})=0, \tag{A2a}$$

$$\lambda\left(\frac{u_r}{r}+\frac{\partial u_r}{\partial r}\right)+2\mu\frac{\partial u_r}{\partial r}-\tau_{rr}=0, \tag{A2b}$$

$$\lambda\left(\frac{u_r}{r}+\frac{\partial u_r}{\partial r}\right)+2\mu\frac{u_r}{r}-\tau_{\theta\theta}=0, \tag{A2c}$$

$$\lambda\left(\frac{u_r}{r}+\frac{\partial u_r}{\partial r}\right)-\tau_{zz}=0. \tag{A2d}$$

The solution to the system of coupled equations in domain $\mathscr{D}_J$ is written as

$$u_r=\left(\frac{r}{r_{J+1}}B_J+\frac{r_J}{r}\right)A_J, \tag{A3a}$$

$$\tau_{rr}=\left(\frac{2(\lambda_J+\mu_J)}{r_{J+1}}B_J-\frac{2\mu_J r_J}{r^2}\right)A_J, \tag{A3b}$$

$$\tau_{\phi\phi}=\left(\frac{2(\lambda_J+\mu_J)}{r_{J+1}}B_J+\frac{2\mu_J r_J}{r^2}\right)A_J, \tag{A3c}$$

$$\tau_{zz}=\left(\frac{2\lambda_J}{r_{J+1}}B_J\right)A_J, \tag{A3d}$$

by which the elastostatic field distribution in the domain $\mathscr{D}_J$ is determined once we have obtained A_J and B_J. Upon substituting Eqs. (A3a) and (A3b) into Eq. (16), the elastostatic radial stiffness in the bounded annular region $\mathscr{D}_J$ is found to be

$$\eta=\frac{2\mu_J(r_J/r)-2(\lambda_J+\mu_J)(r/r_{J+1})B_J}{(r_J/r)+(r/r_{J+1})B_J},$$

$$\text{for } r_J\leqslant r\leqslant r_{J+1}. \tag{A4}$$

Both u_r and τ_{rr} are continuous across the interfaces between the annular domains and, therefore, we have $\lim_{r\uparrow r_{J+1}}\eta(r)=\lim_{r\downarrow r_{J+1}}\eta(r)=\eta_{J+1}$, which, in view of Eq. (A4), leads to

$$B_J=\frac{r_J(2\mu_J-\eta_{J+1})}{r_{J+1}(2\lambda_J+2\mu_J+\eta_{J+1})}. \tag{A5}$$

Since the field quantities are to remain bounded throughout the formation, we have $B_N=0$ and, hence, $\eta_N=2\mu_N=2\mu$. Combining Eqs. (A4) and (A5), we arrive at the backward recurrence scheme

$$\begin{aligned}&\eta_N=2\mu_N=2\mu,\\ &B_J=\frac{r_J(2\mu_J-\eta_{J+1})}{r_{J+1}(2\lambda_J+2\mu_J+\eta_{J+1})},\\ &\eta_J=2\frac{\mu_J-(\lambda_J+\mu_J)(r_J/r_{J+1})B_J}{1+(r_J/r_{J+1})B_J},\\ &\text{for}\quad J=N-1,\ldots,1,\end{aligned} \tag{A6}$$

which is used to obtain the elastostatic radial stiffness at the inner borehole wall.

Next, the amplitude of the traction is transferred from the inner to the outer borehole wall according to

$$\tau_{rr}(r_N)=T\tau_{rr}(r_1). \tag{A7}$$

Using Eq. (A3b) the traction-transfer coefficient is found to be

$$T=\prod_{J=1}^{N-1}\frac{(\lambda_J+\mu_J)B_J-\mu_J(r_J/r_{J+1})}{(\lambda_J+\mu_J)B_J-\mu_J(r_{J+1}/r_J)}. \tag{A8}$$

APPENDIX B: A MOVING SOURCE REPRESENTATION FOR THE VECTOR AND TENSOR POTENTIALS

With the aid of Eqs. (17a) and (17b), the elastodynamic vector and tensor potentials are written as

$$\hat{A}_k(\mathbf{x})=-\delta_{m\mu}\int_{\mathbf{x}'\in\partial\mathscr{B}_S^+}\hat{G}_{km}(\mathbf{x}-\mathbf{x}')\nu_\mu\hat{\tau}(x_3')dA, \tag{B1a}$$

$$\hat{W}_{kmij}(\mathbf{x})=-\frac{sb_S^+}{2\mu}\Delta_{ijk\mu}\int_{\mathbf{x}'\in\partial\mathscr{B}_S^+}\hat{G}_{km}(\mathbf{x}-\mathbf{x}')\times\nu_\kappa\nu_\mu\hat{\tau}(x_3')dA, \tag{B1b}$$

respectively. To approximate these surface integrals by line integrals along the borehole axis, we replace the Green's

tensor by the leading terms of its Taylor expansion about a point on the borehole axis according to

$$\hat{G}_{km}|_{\mathbf{x}'\in\partial\mathscr{B}_S^+}=\hat{G}_{km}|_{\mathbf{x}'\in\mathscr{L}_S}+b_S^+\nu_\lambda\,\partial'_\lambda\hat{G}_{km}|_{\mathbf{x}'\in\mathscr{L}_S}$$

$$+O[s^2(b_S^+)^2/c_S^2]$$

$$+O[(b_S^+)^2/|\mathbf{x}-\mathbf{x}'|^2]$$

$$\approx(1-b_S^+\nu_\lambda\,\partial_\lambda)\hat{G}_{km}|_{\mathbf{x}'\in\mathscr{L}_S}. \tag{B2}$$

Since the radius of the borehole is much smaller than the distance between the source borehole and the receiver borehole, this approximation amounts to neglecting the travel time across a cross section of the borehole. Next, we observe that the amplitude $\hat{\tau}$ of the traction at $\partial\mathscr{B}_S^+$ depends on x_3' and s only and employ the identities $\oint\nu_k\,dl=0$, $\oint\nu_m\nu_n\,dl=\pi b_S^+(\delta_{mn}-\delta_{m3}\delta_{n3})$, and $\oint\nu_k\nu_m\nu_n\,dl=0$, where the integrations are carried out along a cross-sectional circular boundary. As a consequence, Eq. (B1) reduces to

$$\hat{A}_k=-\Omega_S^+\delta_{m\mu}\,\partial_\mu\hat{\Phi}_{km}, \tag{B3a}$$

$$\hat{W}_{kmij}=(s/2\mu)\Omega_S^+\Delta_{ij\kappa\kappa}\hat{\Phi}_{km}, \tag{B3b}$$

in which $\Omega_S^+=\pi(b_S^+)^2$ and

$$\hat{\Phi}_{km}=\int_{\mathbf{x}'\in\mathscr{L}_S}\hat{G}_{km}(\mathbf{x}-\mathbf{x}')[-\hat{\tau}(x_3')]dx_3'. \tag{B4}$$

Next, we substitute the expression for the Green's tensor given by Eq. (24) into Eq. (B4) so as to express Eq. (24) in terms of the scalar potentials $\hat{\Psi}_{P,S}$ according to

$$\hat{\Phi}_{km}=\left(\frac{1}{c_S^2}\delta_{km}-\frac{1}{s^2}\partial_k\partial_m\right)\hat{\Psi}_S+\frac{1}{s^2}\partial_k\partial_m\hat{\Psi}_P. \tag{B5}$$

Using the explicit expressions for the vector and tensor potentials given by Eqs. (B3)–(B5) in Eq. (21), the particle velocity in the formation becomes

$$\hat{v}_k=-\frac{\Omega_S^+ s}{\rho^s}\left(2\delta_{m\kappa}\partial_\kappa+\frac{\lambda}{\mu}\partial_m\right)\hat{\Phi}_{km}$$

$$=\frac{\Omega_S^+ s}{\rho^s}\left[-2\left(\frac{1}{c_S^2}\delta_{k\kappa}\,\partial_\kappa-\frac{1}{s^2}\partial_\kappa\partial_\kappa\partial_k\right)\hat{\Psi}_S-\frac{\lambda}{\mu}\left(\frac{1}{c_S^2}\right.\right.$$

$$\left.\left.-\frac{1}{s^2}\partial_m\partial_m\right)\partial_k\hat{\Psi}_S-\frac{1}{s^2}\left(2\,\partial_\kappa\partial_\kappa+\frac{\lambda}{\mu}\partial_m\partial_m\right)\partial_k\hat{\Psi}_P\right]. \tag{B6}$$

With the aid of the relation $2+\lambda/\mu=c_P^2/c_S^2$ and the property $\partial_\kappa\partial_\kappa\hat{\Psi}_{P,S}=(-\partial_3\partial_3+s^2/c_{P,S}^2)\hat{\Psi}_{P,S}$ outside the source point, we eliminate most of the derivatives with respect to the horizontal coordinates, thus arriving at Eq. (27a). Upon using Eq. (21b) we obtain the expression for the stress, given by Eq. (27b).

APPENDIX C: DECOMPOSITION OF THE EXPRESSION FOR THE ACOUSTIC PRESSURE INTO ITS ELEMENTARY CONSTITUENTS

In this Appendix we derive the simplified expression for the Laplace–transform-domain acoustic pressure given by Eqs. (39)–(41).

As the point of departure we shall rewrite the boundary integral representation for the acoustic pressure given by Eq. (34) in terms of a line integral representation. To this end, we replace $\hat{v}_i^{\text{in}}(\mathbf{x})$ and $\hat{\tau}_{pq}^{\text{in}}(\mathbf{x})$ by the leading terms of their Taylor expansions about a point $\mathbf{x}$ on the borehole axis according to

$$\hat{v}_i^{\text{in}}|_{\mathbf{x}'\in\partial\mathscr{B}_R^+}=(1+b_R^+\nu_\lambda\,\partial_\lambda)\hat{v}_i^{\text{in}}|_{\mathbf{x}'\in\mathscr{L}_R}, \tag{C1a}$$

$$\hat{\tau}_{pq}^{\text{in}}|_{\mathbf{x}'\in\partial\mathscr{B}_R^+}=(1+b_R^+\nu_\lambda\,\partial_\lambda)\hat{\tau}_{pq}^{\text{in}}|_{\mathbf{x}'\in\mathscr{L}_R}, \tag{C1b}$$

respectively. This approximation is analogous to the one used in Eq. (B2) and amounts to neglecting the travel time across a cross section of the receiving borehole. Upon substituting Eqs. (17) and (C1) into Eq. (34) and employing the identities $\oint\nu_k\,dl=0$, $\oint\nu_m\nu_n\,dl=\pi b_R^+(\delta_{mn}-\delta_{m3}\delta_{n3})$, and $\oint\nu_k\nu_m\nu_n\,dl=0$, where the integrations are carried out along a cross-sectional circular boundary, the line integral Eq. (35) results.

We resume our derivation with a change of the variables of integration in Eq. (37) according to $x_3'=\zeta_1+x_3^S$ and $x_3=\zeta_2+x_3^R$. As a consequence, we have $dx_3'=d\zeta_1$ and $dx_3=d\zeta_2$, respectively. In terms of these new variables, the source and receiver levels are $\zeta_1=0$ and $\zeta_2=0$, respectively. Furthermore, the difference vector $\mathbf{x}-\mathbf{x}'$ has the coordinates $(d,0,z+\zeta_2-\zeta_1)$ relative to our original coordinate system. Having used the property of the scalar Green's functions $\hat{G}_{P,S}$ that they depend on ζ_1 and ζ_2 only through their difference $\zeta_2-\zeta_1$, implying that $\partial_{\zeta_1}\hat{G}_{P,S}=-\partial_{\zeta_2}\hat{G}_{P,S}$, we arrive at

$$\hat{p}^T(\mathbf{x}^R)=4\Omega_S^+\Omega_R^+T_ST_R\frac{s}{\rho^s}\int_{\zeta_2\in\mathscr{L}_R}\int_{\zeta_1\in\mathscr{L}_S}\hat{p}^S(\zeta_1$$

$$+x_3^S)\hat{p}^R(\zeta_2+x_3^R)\left\{\left[-\left(\frac{1}{c_S^2}+\frac{1}{s^2}\partial_{\zeta_1}\partial_{\zeta_2}\right)\right.\right.$$

$$\left.\times\partial_{\zeta_1}\partial_{\zeta_2}\hat{G}_S(\mathbf{x}-\mathbf{x}')\right]+\left[s^2\left(\frac{1}{2c_S^2}\right.\right.$$

$$\left.\left.\left.+\frac{1}{s^2}\partial_{\zeta_1}\partial_{\zeta_2}\right)^2\hat{G}_P(\mathbf{x}-\mathbf{x}')\right]\right\}d\zeta_2\,d\zeta_1. \tag{C2}$$

Next, we substitute Eq. (38) into Eq. (C2) and repeatedly employ integration by parts until all derivatives with respect to ζ_1 and ζ_2 have been eliminated. As a result, the expression for the acoustic pressure reduces to

$$\hat{p}^T(\mathbf{x}^R)=\frac{\Omega_S^+\Omega_R^+}{\Omega_S^-\Omega_R^-}T_S T_R\frac{\rho_S^f\rho_R^f}{\rho^s}s^3\hat{Q}c_{BS}c_{BR}\Bigg[\frac{4}{s^2c_{BS}c_{BR}}(\hat{G}_P-\hat{G}_S)+\left(\frac{1}{c_{BS}c_{BR}}+\frac{1}{2c_S^2}\right)^2(\hat{\sigma}_P^{++}+\hat{\sigma}_P^{--})+\left(\frac{1}{c_{BS}c_{BR}}-\frac{1}{2c_S^2}\right)^2$$
$$\times(\hat{\sigma}_P^{+-}+\hat{\sigma}_P^{-+})-\frac{2}{sc_{BR}c_{BS}^2}[\hat{\chi}_P(z,c_{BS})+\hat{\chi}_P(-z,c_{BS})]+\frac{2}{sc_{BS}c_{BR}^2}[\hat{\chi}_P(z,c_{BR})+\hat{\chi}_P(-z,c_{BR})]$$
$$-\left(\frac{1}{c_{BS}^2c_{BR}^2}+\frac{1}{c_{BS}c_{BR}c_S^2}\right)(\hat{\sigma}_S^{++}+\hat{\sigma}_S^{--})-\left(\frac{1}{c_{BS}^2c_{BR}^2}-\frac{1}{c_{BS}c_{BR}c_S^2}\right)(\hat{\sigma}_S^{+-}+\hat{\sigma}_S^{-+})-\frac{2}{sc_{BR}c_{BS}^2}$$
$$\times[\hat{\chi}_S(z,c_{BS})+\hat{\chi}_S(-z,c_{BS})]-\frac{2}{sc_{BS}c_{BR}^2}[\hat{\chi}_S(z,c_{BR})+\hat{\chi}_S(-z,c_{BR})]\Bigg], \tag{C3}$$

in which

$$\hat{\sigma}_{P,S}^{\pm\pm}(d,z,c_{BS},c_{BR})$$
$$=\int_{\zeta_2=-\infty}^{\infty}\int_{\zeta_1=-\infty}^{\infty}\hat{G}_{P,S}(d,0,z+\zeta_2-\zeta_1)$$
$$\times[\exp(\mp s\zeta_1/c_{BS})H(\pm\zeta_1)][\exp(\mp s\zeta_2/c_{BR})$$
$$\times H(\pm\zeta_2)]d\zeta_2\,d\zeta_1 \tag{C4}$$

are the remaining double integral constituents along the two borehole axes. The first set of signs on the left-hand side of Eq. (C4) indicates down- or upgoing tube modes in the source borehole; the second set of signs on the left-hand side of Eq. (C4) indicates up- or downgoing tube modes in the receiving borehole. The compressional- and shear-wave single integral constituents

$$\hat{\chi}_{P,S}(z,c)=\int_{\zeta=0}^{\infty}\hat{G}_{P,S}(d,0,z-\zeta)\exp\left(-\frac{s\zeta}{c}\right)d\zeta \tag{C5}$$

result from the contributions of the end points in either borehole, while the direct compressional- and shear-wave constituents $\hat{G}_{P,S}$ result from the contribution of the end points in the two boreholes.

Each of the double integrals $\hat{\sigma}_{P,S}^{++}$ can be written in terms of single integrals by using integration by parts. For example, we rewrite $\hat{\sigma}_P^{++}$ as

$$\hat{\sigma}_P^{++}=\int_{\zeta_1=0}^{\infty}\int_{\zeta_2=0}^{\infty}\hat{G}_P(d,0,z+\zeta_2-\zeta_1)\exp\left(-\frac{s\zeta_1}{c_{BS}}\right)\exp\left(-\frac{s\zeta_2}{c_{BR}}\right)d\zeta_1\,d\zeta_2$$
$$=\frac{c_{BR}}{s}\hat{\chi}_P(z,c_{BS})-\frac{c_{BR}}{s}\int_{\zeta_1=0}^{\infty}\int_{\zeta_2=0}^{\infty}\partial_{\zeta_1}\hat{G}_P(d,0,z+\zeta_2-\zeta_1)\exp\left(-\frac{s\zeta_1}{c_{BS}}\right)\exp\left(-\frac{s\zeta_2}{c_{BR}}\right)d\zeta_1\,d\zeta_2$$
$$=\frac{c_{BR}}{s}\hat{\chi}_P(z,c_{BS})+\frac{c_{BR}}{s}\int_{\zeta_2=0}^{\infty}\hat{G}_P(d,0,z+\zeta_2)\exp\left(-\frac{s\zeta_2}{c_{BR}}\right)d\zeta_2$$
$$+\frac{c_{BR}}{s}\int_{\zeta_1=0}^{\infty}\int_{\zeta_2=0}^{\infty}-\frac{s}{c_{BS}}\hat{G}_P(d,0,z+\zeta_2-\zeta_1)\exp\left(-\frac{s\zeta_1}{c_{BS}}\right)\exp\left(-\frac{s\zeta_2}{c_{BR}}\right)d\zeta_1\,d\zeta_2$$
$$=\frac{c_{BR}}{s}[\hat{\chi}_P(z,c_{BS})+\hat{\chi}_P(-z,c_{BR})]-\frac{c_{BR}}{c_{BS}}\hat{\sigma}^{++}, \tag{C6}$$

by virtue of which we can express the double integral $\hat{\sigma}_P^{++}$ in terms of the single integral contributions. For the generic case in which both of the tube-mode wave speeds are different, we obtain

$$\hat{\sigma}_{P,S}^{++}=\frac{c_{BS}c_{BR}}{s(c_{BS}+c_{BR})}[\hat{\chi}_{P,S}(z,c_{BS})+\hat{\chi}_{P,S}(-z,c_{BR})],$$

$$\hat{\sigma}_{P,S}^{--}=\frac{c_{BS}c_{BR}}{s(c_{BS}+c_{BR})}[\hat{\chi}_{P,S}(-z,c_{BS})+\hat{\chi}_{P,S}(z,c_{BR})], \tag{C7}$$

$$\hat{\sigma}_{P,S}^{+-}=\frac{c_{BS}c_{BR}}{s(c_{BS}-c_{BR})}[\hat{\chi}_{P,S}(z,c_{BS})-\hat{\chi}_{P,S}(z,c_{BR})],$$

$$\hat{\sigma}_{P,S}^{-+}=\frac{c_{BS}c_{BR}}{s(c_{BS}-c_{BR})}[\hat{\chi}_{P,S}(-z,c_{BS})-\hat{\chi}_{P,S}(-z,c_{BR})].$$

Substitution of Eqs. (C7) into Eq. (C3) leads, after rearranging the terms, to the elementary expression for the acoustic pressure given by Eq. (39).

APPENDIX D: DERIVATION OF THE TIME-DOMAIN ELEMENTARY CONSTITUENTS

To derive the expressions for the space-time-domain elementary constituents $\chi_{P,S}$, we rewrite Eq. (41) as

$$\hat{\chi}_{P,S}(z,c_B)=\int_{\zeta=0}^{\infty}\frac{\exp[-s\tau(\zeta)]}{4\pi D(\zeta)}\,d\zeta, \tag{D1}$$

in which

$$D(\zeta)=[d^2+(z-\zeta)^2]^{1/2}, \tag{D2a}$$

$$\tau(\zeta)=\zeta/c_B+D(\zeta)/c_{P,S}. \tag{D2b}$$

The objective is to take τ as the new variable of integration. To this end, we have to investigate whether the Jacobian

$$\partial_\zeta\tau=(c_B)^{-1}-(z-\zeta)[c_{P,S}D(\zeta)]^{-1} \tag{D3}$$

vanishes for a certain $\zeta=\zeta_m\in(0,\infty)$. For $c_B<c_{P,S}$ the Jacobian is positive definite, implying that τ is monotonic on $(0,\infty)$. For $c_B>c_{P,S}$, we can solve $\partial_\zeta\tau=0$ for $\zeta=\zeta_m$, which yields

$$\zeta_m=\zeta_m(c_{P,S})=z-d(c_B^2/c_{P,S}^2-1)^{-1/2}. \tag{D4}$$

So, $\zeta=\zeta_m\in(0,\infty)$ if

$$\begin{aligned}&c_B>c_{P,S},\\ &z/d=\cot(\theta)>(c_B^2/c_{P,S}^2-1)^{-1/2}=\cot(\theta_C),\end{aligned} \tag{D5}$$

where $\theta_C=\pi/2-\alpha_C$, with $\alpha_C=\alpha_C(c_{P,S},c_B)$ being the critical angle, i.e., the angle of conical refraction. If the conditions stated in Eq. (D5) are met, the body wave is preceded by a conical wave. The latter's arrival time is given by

$$\begin{aligned}t_C&=\tau(\zeta_m)\\ &=|z|/c_B+d(c_{P,S}^{-2}-c_B^{-2})^{1/2}\\ &=\begin{cases}t_{P,S}\cos(\theta_C-\theta), & \text{for } \theta<\theta_C,\\ t_{P,S}\cos(\theta+\theta_C-\pi), & \text{for } \theta>\theta_C-\pi.\end{cases}\end{aligned} \tag{D6}$$

For postcritical offsets, we consider Eq. (D1) to consist of the sum of two integral contributions with their intervals of integration being $[0,\zeta_m)$ and (ζ_m,∞), respectively. On these intervals, the solution of Eq. (D2) for $\zeta=\zeta(\tau)$ is given by

$$\zeta=\frac{\tau/c_B+z/c_{P,S}\pm T/c_{P,S}}{c_{P,S}^{-2}-c_B^{-2}}\quad\begin{cases}+ & \text{for } \zeta\in(\zeta_m,\infty),\\ - & \text{for } \zeta\in[0,\zeta_m),\end{cases} \tag{D7}$$

in which

$$T(\tau,d,z,c_B,c_{P,S})=[(\tau-z/c_B)^2-d^2(c_{P,S}^{-2}-c_B^{-2})]^{1/2}. \tag{D8}$$

As a consequence of changing the variable of integration from ζ to τ, we have $d\zeta=(\partial_\zeta\tau)^{-1}\,d\tau$. Upon using Eqs. (D2), (D3), and (D7), the Jacobian of the transformation is found to be

$$(\partial_\zeta\tau)^{-1}=\frac{\pm D(\zeta)}{T}\quad\begin{cases}+ & \text{for } \zeta\in(\zeta_m,\infty),\\ - & \text{for } \zeta\in[0,\zeta_m).\end{cases} \tag{D9}$$

With the aid of Eq. (D9), we rewrite Eq. (D1) as

$$\begin{aligned}\hat{\chi}_{P,S}(z,c_B)&=\left(\int_{\tau=t_{P,S}}^{t_C}+\int_{\tau=t_C}^{\infty}\right)\frac{\exp(-s\tau)}{4\pi D}(\partial_\zeta\tau)^{-1}\,d\tau\\ &=\left(\int_{\tau=t_C}^{t_{P,S}}+\int_{\tau=t_C}^{\infty}\right)\frac{\exp(-s\tau)}{4\pi T}\,d\tau.\end{aligned} \tag{D10}$$

For precritical offsets τ increases monotonically with increasing ζ, implying that conical waves do not occur. An analysis similar to the one above then leads to

$$\hat{\chi}_{P,S}(z,c_B)=\int_{\tau=t_{P,S}}^{\infty}\frac{\exp(-s\tau)}{4\pi T}\,d\tau. \tag{D11}$$

In view of Lerch's theorem, we infer from Eqs. (D8), (D10), and (D11) that the space-time-domain constituents $\chi_{P,S}$ are given by Eq. (43).

APPENDIX E: THE FAR-FIELD ASYMPTOTIC REPRESENTATION FOR THE PARTICLE VELOCITY IN THE FORMATION

The expressions for the particle velocity measured by a receiver inside the solid formation are given by Eq. (27a), in terms of the scalar potentials given by Eq. (26), which with the aid of Eqs. (6), (15), and (18) are rewritten as

$$\hat{\Psi}_{P,S}=T_S(\hat{Q}\rho^f c_B/2\Omega_s^-)[\hat{\chi}_{P,S}(z,c_B)+\hat{\chi}_{P,S}(-z,c_B)]. \tag{E1}$$

In order to compare Eq. (27a) with the far-field expressions for the particle displacement in fast formations obtained by Lee and Balch,[8] it suffices to investigate the leading order of the asymptotic expansion of the Laplace integral

$$\hat{\chi}_{P,S}(z,c_B)=\int_{\zeta=0}^{\infty}\frac{\exp[-s\tau(\zeta)]}{4\pi D(\zeta)}\,d\zeta, \tag{E2}$$

for large s. To distinguish between the conical- and body-wave contributions, we write

$$\hat{\chi}_{P,S}=\hat{\chi}_{P,S}^C+\hat{\chi}_{P,S}^B. \tag{E3}$$

For postcritical offsets and z positive, τ assumes its minimum $\tau=t_C(c_{P,S})$ at the critical point $\zeta=\zeta_m(c_{P,S})$, thus giving rise to a conical-wave contribution. Applying Laplace's method (cf. Bender and Orszag[27]), the leading term of the asymptotic expansion for a conical wave is found to be

$$\hat{\chi}_{P,S}^C(z,c_B)\sim\begin{cases}\dfrac{\exp(-st_C)}{2\pi\sqrt{2d}}\sqrt{\dfrac{\pi}{s}}\,(c_{P,S}^{-2}-c_B^{-2})^{-1/4},\\ \quad\text{for } \theta<\theta_C(c_{P,S})\\ 0,\quad\text{otherwise,}\end{cases} \tag{E4}$$

where $t_C(c_{P,S})$ is the wave speed of the pertaining conical wave, given by Eq. (44). The leading term of the asymptotic expansion for a body-wave contribution becomes

$$\hat{\chi}^B_{P,S}(z,c_B)\sim\frac{\exp(-st_{P,S})}{4\pi s}\left(\frac{R}{c_B}-\frac{z}{c_{P,S}}\right)^{-1},$$

$$\text{for } \theta\neq\theta_C(c_S), \tag{E5}$$

which can be obtained using integration by parts.

In view of the symmetry in z, we henceforth consider z to be positive without loss of generality. Let us introduce the unit vectors ξ, which is oriented along the vector $(\mathbf{x}^R-\mathbf{x}^S)$, and $\Xi=\Xi(c_{P,S})$, which is at an angle θ_C with the vertical (see Fig. 3). The unit vectors perpendicular to ξ and Ξ are denoted as $\xi^\perp$ and $\Xi^\perp$, respectively. From Eqs. (D6), (E4), and (E5), we infer that in the far-field region, the spatial derivatives are replaced by multiplications, according to

$$\partial_m\hat{\chi}^C_{P,S}\sim-(s/c_{P,S})\Xi_m(c_{P,S})\hat{\chi}^C_{P,S},\quad \text{for } \theta<\theta_C(c_{P,S}), \tag{E6a}$$

$$\partial_m\hat{\chi}^B_{P,S}\sim-(s/c_{P,S})\xi_m\hat{\chi}^B_{P,S}, \tag{E6b}$$

which follows after having discarded all but the leading terms in s. Upon substituting Eqs. (E4)–(E6) into Eq. (27a), we arrive at an asymptotic representation for the particle velocity in the formation for large s.

Now, the space-time-domain particle velocity in the formation is expressed in terms of its compressional- and shear-, conical- and body-wave components according to

$$v_k=v_k^{CP}+v_k^{BP}+v_k^{CS}+v_k^{BS}. \tag{E7}$$

Next, we make use of the transformation rules

$$s\rightarrow\partial_t, \tag{E8a}$$

$$\hat{Q}\exp(-st_{P,S})/s\rightarrow Q(t)\overset{t}{*}H(t-t_{P,S}), \tag{E8b}$$

$$\hat{Q}\exp(-st_C)\sqrt{\pi/s}\rightarrow Q(t)\overset{t}{*}[(t-t_C)^{-1/2}H(t-t_C)], \tag{E8c}$$

and substitute Eqs. (E1)–(E7) into Eq. (27a), so as to obtain the space-time-domain asymptotic expansion for the pertaining components of the particle velocity in the formation given by

$$v_k^{CP;BP;CS;BS}\sim T_S(\rho^f\Omega_S^+/4\pi\rho^s\Omega_S^-)\partial_t^2Q\overset{t}{*}\Gamma_k^{CP;BP;CS;BS} \tag{E9}$$

in which the compressional- and shear-, conical- and body-wave Green's functions are given by

$$\Gamma_k^{CP}\sim c_B\frac{c_S^{-2}-2c_B^{-2}}{(c_S^{-2}-c_B^{-2})^{1/4}}\frac{H(t-t_C(c_P))}{c_P\sqrt{2d}[t-t_C(c_P)]^{1/2}}\Xi_k(c_P),$$

$$\text{for } \theta<\theta_C(c_P), \tag{10a}$$

$$\Gamma_k^{BP}\sim\frac{1-2(c_S/c_B)^2\cos^2(\theta)}{(c_S/c_B)^2-(c_S/c_P)^2\cos^2(\theta)}\frac{H(t-t_P)}{c_PR}\xi_k,$$

$$\text{for } \theta\neq\theta_C(c_P), \tag{E10b}$$

$$\Gamma_k^{CS}\sim2(c_S^{-2}-c_B^{-2})^{1/4}\frac{H(t-t_C(c_S))}{c_S\sqrt{2d}[t-t_C(c_S)]^{1/2}}\Xi_k^\perp(c_S),$$

$$\text{for } \theta<\theta_C(c_S), \tag{E10c}$$

$$\Gamma_k^{BS}\sim\frac{2\sin(\theta)\cos(\theta)}{(c_S/c_B)^2-\cos^2(\theta)}\frac{H(t-t_S)}{c_SR}\xi_k^\perp,$$

$$\text{for } \theta\neq\theta_C(c_S), \tag{E10d}$$

respectively. Earlier, Lee and Balch[8] obtained the far-field expression for the particle displacement in a fast formation due to the action of a point source of volume injection located on the axis of a fluid-filled open borehole. To show that their expressions agree with the far-field expressions for the particle velocity in the precritical regions given by Eq. (E10), we have to carry out the substitutions

$$v_k\rightarrow\partial_tu_k, \tag{E11a}$$

$$Q\rightarrow V_0\,\partial_tg(t), \tag{E11b}$$

$$T_s\rightarrow1, \tag{E11c}$$

$$\Omega_S^+/\Omega_S^-\rightarrow1, \tag{E11d}$$

where u_k is the particle displacement, while V_0 and $g(t)$ are the symbols used by Lee and Balch to indicate the total injected volume and the source signature, respectively.

[1] J. E. White and R. L. Sengbush, "Shear waves from explosive sources," Geophysics **28**, 1001–1019 (1963).
[2] J. A. de Bruin and W. Huizer, "Radiation from waves in boreholes," Scientific Drilling **1**, 3–10 (1992).
[3] N. Cheng, Z. Zhu, C. H. Cheng, and M. N. Toksöz, "Experimental and finite difference modeling of borehole Mach waves," EAEG Expanded Abstracts, paper P070, Paris (1992).
[4] J. N. Albright and P. A. Johnson, "Cross-borehole observation of mode conversion from borehole Stoneley waves to channel waves at a coal layer," Geophys. Prosp. **38**, 607–620 (1990).
[5] M. H. Worthington, "Cross-well continuity logging using Stoneley waves at the Whitchester borehole test site," EAEG Expanded Abstracts, paper B039, Florence (1991).
[6] L. R. Lines, K. R. Kelly, and J. Queen, "Channel waves in cross-borehole data," Geophysics **57**, 334–342 (1992).
[7] C. E. Krohn, "Cross-well continuity logging using seismic guided waves," 60th Annual International Meeting, Society of Exploration Geophysicists, Expanded Abstracts, 43–46 (1990).
[8] M. W. Lee and A. H. Balch, "Theoretical seismic wave radiation from a fluid-filled borehole," Geophysics **47**, 1308–1314 (1982).
[9] J. A. Meredith, "Numerical and analytical modeling of downhole seismic sources: The near and far field," Ph.D. thesis, Massachusetts Institute of Technology (1990).
[10] M. W. Lee, A. H. Balch, and K. R. Parrot, "Radiation from a downhole airgun source," Geophysics **49**, 27–36 (1984).
[11] M. W. Lee, "Low-frequency radiation from point sources in a fluid-filled borehole," Geophysics **51**, 1801–1807 (1986).
[12] G. A. Winbow, "Seismic sources in open and cased boreholes," Geophysics **56**, 1040–1050 (1991).
[13] A. Track and F. Daube, "Borehole coupling in cross-well wave propagation," EAEG Expanded Abstracts, paper B026, Paris (1992).
[14] P. A. Heelan, "Radiation from a cylindrical source of finite length," Geophysics **18**, 685–696 (1953).
[15] A. Ben-Menahem and S. Kostek, "The equivalent force system of a monopole source in a fluid-filled open borehole," Geophysics **56**, 1477–1481 (1990).
[16] A. L. Kurkjian, B. P. de Hon, J. E. White, A. T. de Hoop, and T. L. Marzetta, "A moving point mechanism representation for low frequency monopole borehole sensors," EAEG Expanded Abstracts, paper P074, Paris (1992).
[17] A. L. Kurkjian, H. Schmidt, J. E. White, T. L. Marzetta, and C. Chouzenoux, "Numerical modeling of cross-well seismic monopole sensor data," 62th Annual International Meeting, Society of Exploration Geophysicists, Expanded Abstracts, 141–144 (1992).
[18] R. L. Gibson, Jr., "Modeling Mach wave Propagation between Bore-

holes in Layered Media," EAEG Expanded Abstracts, paper B027, Paris (1992).
[19] M. Schoenberg, "Fluid and solid motion in the neighborhood of a fluid-filled borehole due to the passage of a low-frequency elastic plane wave," Geophysics **51**, 1191–1205 (1986).
[20] J.-L. Boelle, M. Dietrich, and B. Paternoster, "Coupled tube waves between two boreholes: a theoretical approach," EAEG Expanded Abstracts, paper C017, Paris (1992).
[21] J. E. White, *Underground Sound—Application of Seismic Waves* (Elsevier, New York, 1983), Chap. 5, pp. 145–147.
[22] T. L. Marzetta, and M. Schoenberg, "Tube waves in cased boreholes," 55th Annual International Meeting, Society of Exploration Geophysicists, Expanded Abstracts, 34–36 (1985).
[23] A. T. de Hoop, "Representation theorems for the displacement in an elastic solid and their application to elastodynamic diffraction theory," Ph.D. thesis, Delft University of Technology (1958).
[24] A. T. de Hoop, "A time-domain energy theorem for the scattering of plane elastic waves," Wave Motion **7**, 569–577 (1985).
[25] A. T. de Hoop, "Reciprocity theorems for acoustic wave fields in fluid/solid configurations," J. Acoust. Soc. Am. **87**, 1932–1937 (1990).
[26] F. J. Harris, "On the use of windows for harmonic analysis with the discrete Fourier Transform," Proc. IEEE **66**, 51–83 (1978).
[27] C. M. Bender and S. A. Orszag, *Advanced Mathematical Methods for Scientists and Engineers* (McGraw-Hill, New York, 1978), Chap. 6, pp. 261–276.